Conference Paper, Published Version

Yahata, Eriko; Kimura, Ichiro; Iwasaki, T.; Shimizu, Yoshikazu; Nelson, J. M.

Comparisons of various CFD models for computing river flows focusing on secondary currents

River Flow 2010 - Dittrich, Koll, Aberle & Geisenhainer (eds) - © 2010 Bundesanstalt für Wasserbau ISBN 978-3-939230-00-7

Comparisons of Various CFD Models for Computing River Flows Focusing on Secondary Currents

Eriko Yahata, Ichiro Kimura, Toshiki Iwasaki & Yasuyuki Shimizu
Hokkaido University, Sapporo, Japan

Jonathan M Nelson
USGS, Sacramento, CA, USA

ABSTRACT: Secondary currents are flows (usually vortices) in a cross section vertically against primary flows. Secondary currents grow significantly in recirculation at abrupt expansions. Computational models for simulating those secondary currents requires are usually 3D (three-dimensional) models because secondary flows are intrinsically three-dimensional. However full 3D models are sometimes not optimal tools on practical point of view because they require the computational heavy load and larger CPU time, though 3D models reproduce flows more accurately and realistically. On the other hand, normal 2D models are much less expensive but it is too simple to replicate secondary currents. In this paper, we examined the applicability of advanced 2D models in which effects of secondary currents are integrated. Such model is likely able to reproduce mean flows of a river with secondary currents though the computational load of the models is competitive with normal 2D models. The performance of the models is validated by comparing the numerical results with measured data in a real river. The USGS performed a flooding experiment in Colorado River in March 2008 and measured stream regime in three-dimension before, during and after the flood. The performances of these 2D models are examined focussing on the secondary current in real river scales through the comparison with the measured data by USGS. The numerical results show that the advanced 2D models can predict reasonably the fundamental features of mean velocity profiles and qualitative aspects of the secondary currents.

Keywords: Numerical simulation, Secondary currents, the Colorado River, plane 2D CFD model

1 INTRODUCTION

1.1 *General*

Secondary currents of the first kind that arise at river bends or recirculation zone are flows (vortices) in a cross section vertically against primary flows due to the local unbalance of pressure gradient and the centrifugal force. The rate of development and movement of the secondary currents closely depends on the complex 3D (three-dimensional) flow features. Therefore simulation model for those secondary currents requires precise modelling of 3D process in eddies. However 3D models are not optimal tools on practical side because the models require heavy load on computers and long CPU time. On the other hand, a normal 2D model, which is often used for practical flow phenomena as well as sediment transport in real rivers, is light loaded but it is too simple to replicate secondary currents.

In this paper, we tried to apply advanced 2D models, in which effects of secondary currents are incorporated through vertical integration, to secondary currents phenomena in real rivers. The advanced 2D models are likely able to reproduce mean flow patterns of a river with secondary currents and their computational load is much less than 3D models. In addition, we can reconstruct three-dimensional flows from calculated mean flows considering assumed velocity profiles in the stream-wise and transverse directions.

The computations are performed under the same conditions of the measured data in Colorado River, USA performed by United States Geological Survey (USGS). We applied 3 different types of depth averaged models and the model performance in each model is discussed through the comparison with the measured data.

1.2 *Flood Experiment by USGS*

In March 2008, an artificial flood experiment was conducted in Colorado River by USGS. The data that measured during this experiment are quite beneficial to verify numerical models focusing on secondary currents as

- detailed 3D flow measurement data in real rivers themselves are difficult to be obtained.
- the ratio of width / depth in the Colorado river is high and secondary currents develop well.
- the measurement site locates in a desert and there is little vegetation in the river channel, so unaffected flows by vegetation can be observed.

The hydrograph of this flood is shown in Figure 1. The hydrograph was composed of a rising limb of about 36 hours, a steady high discharge with duration of about 60 hours, and a falling limb of about 28hours.

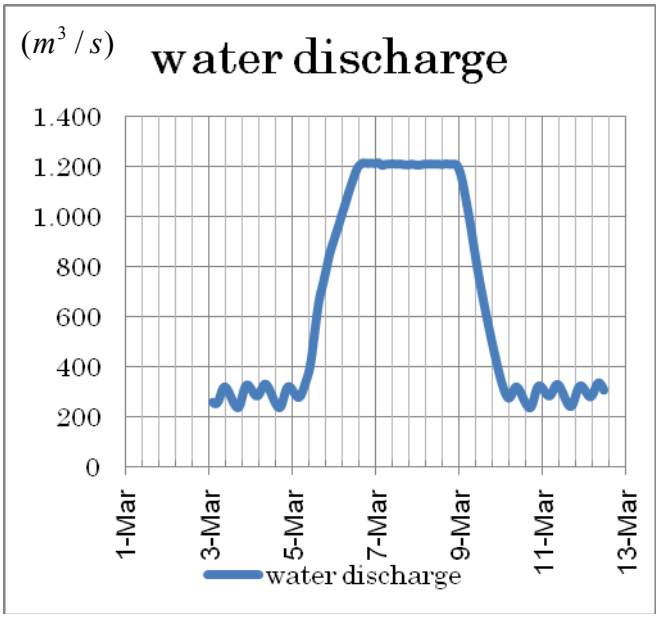

Figure 1 Discharge hydrograph measured at Glen Canyon Dam

Before, during and after the high flow period, measurements were done at several sites along the river by USGS scientists and surveyors (e.g., at river-miles 30, 45, 60, 87). For verifying advanced 2D models (refer to section 2.), data collection focuses on an eddy near River-Mile 45. This area contains two pools (Eminence and Willie Taylor pools) connected by a small rapid/riffle. Data collection in this research includes the following:

1. Multi-beam surveys twice a day
2. ADCP surveys twice a day
3. Suspended-sediment samples daily
4. Pre- and post- high flow bed grain-size surveys
5. Post-high flow trenching of deposits, sedimentology

Velocities were measured at 10m intervals in x and y directions and at 33cm intervals in z direction (x:streamwise direction, y:spanwise direction, z:vertical direction).

The focused place is at 45 river-miles downstream from the dam. (See Figure. 2) There are two pools (side-cavities) around there. In this paper, we consider the upper one which is called Eminence. (See Figure.3)

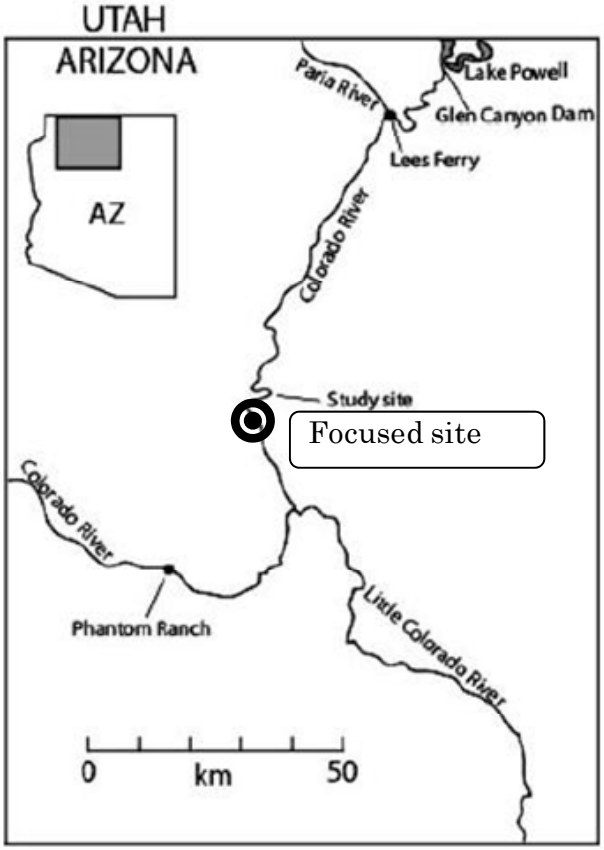

Figure 2 Location map of the Colorado River.

1.3 *Secondary currents at Eminence*

Figure.3 shows measured depth-averaged velocities. A large eddy can be seen around the cavity like area. Figure.4 shows a cross sectional flow pattern along ① cross section which is the closest section to the centre of the large eddy.

Downward flows can be seen near the left and right banks and an upward flow can be seen around the centre part. Those flows indicate generation of secondary current cased by the recirculation around a pool.

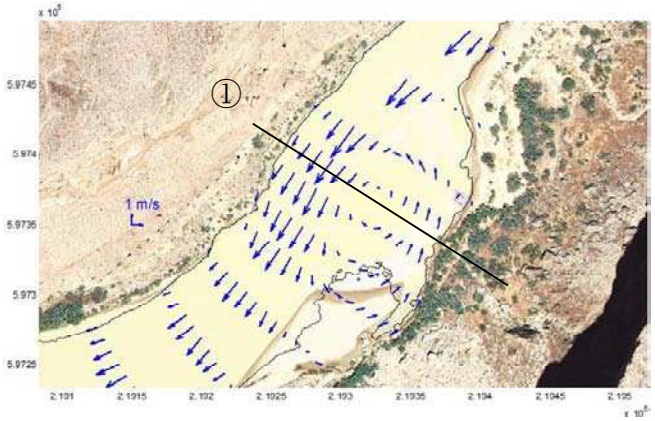

Figure 3 The upper pool which is called Eminence and its measured depth-averaged velocities during the peak flow.

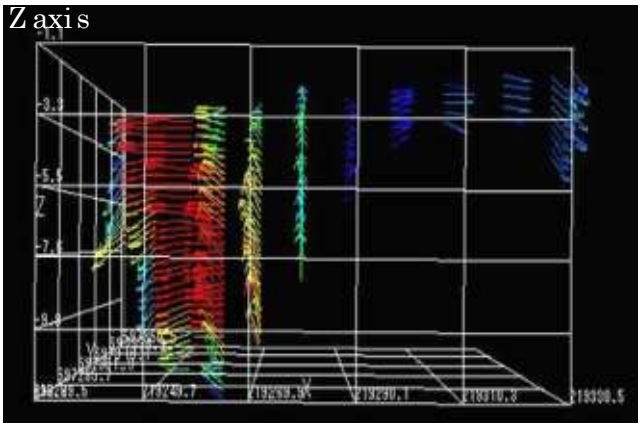

Figure 4 Cross section at ①. Z axis means depth in meter, X axis means X coordinate. Vectors mean velocities.

2 NUMERICAL ANALYSYS METHOD

2.1 *Basic Equations*

The governing equations are composed of depth-averaged continuity and momentum equations. The equations in the Cartesian coordinate are described as follows.

{Continuity equation}

$$\frac{\partial h}{\partial t}+\frac{\partial M}{\partial x}+\frac{\partial N}{\partial y}=0 \tag{1}$$

{Momentum equation in x-direction}

$$\frac{\partial M}{\partial t}+\frac{\partial \beta uM}{\partial x}+\frac{\partial \beta vM}{\partial y}+gh\frac{\partial (h+z_b)}{\partial x}=$$
$$gh\sin\theta-\frac{\tau_{bx}}{\rho}+\frac{\partial -\overline{u'^2}h}{\partial x}+\frac{\partial -\overline{u'v'}h}{\partial y} \tag{2}$$
$$+\nu\left\{\frac{\partial}{\partial x}\left(h\frac{\partial u}{\partial x}\right)+\frac{\partial}{\partial y}\left(h\frac{\partial u}{\partial y}\right)\right\}+S_{cx}$$

{Momentum equation in y-direction}

$$\frac{\partial N}{\partial t}+\frac{\partial \beta uN}{\partial x}+\frac{\partial \beta vN}{\partial y}+gh\frac{\partial (h+z_b)}{\partial y}=$$
$$-\frac{\tau_{by}}{\rho}+\frac{\partial -\overline{v'u'}h}{\partial x}+\frac{\partial -\overline{v'^2}h}{\partial y} \tag{3}$$
$$+\nu\left\{\frac{\partial}{\partial x}\left(h\frac{\partial v}{\partial x}\right)+\frac{\partial}{\partial y}\left(h\frac{\partial v}{\partial y}\right)\right\}+S_{cy}$$

where, (x,y):spatial coordinate, t:time, h: water depth, (u, v):depth-averaged velocity components in (x, y) directions, (M, N):fluxes in (x, y) direction defined as(hu, hv), (u', v'): turbulence velocities in (x, y) directions, $-u'_iu'_j$: depth-averaged Reynolds stress tensor, v: dynamic viscosity coefficient, $\sin\theta$:bed slope, f: friction coefficient (friction of Reynolds number), (τ_{bx},τ_{by}): bed friction stress vector, β:momentum coefficient, θ_f: angle between stream line and x-axis, (D_x, D_y): eddy diffusivity coefficients in (x, y) directions, (ι_{bx}, ι_{by}): bottom shear-stresses in (x, y) directions, S_{cx}, S_{cy}, S_{cc}: additional terms due to the secondary currents.

Components of the bottom shear-stress vector are evaluated by

$$\tau_{bx}=\frac{fpu}{2}\sqrt{u^2+v^2};\ \tau_{by}=\frac{fpv}{2}\sqrt{u^2+v^2} \tag{6}$$

where f =friction factor related to local Reynolds number $R_e'\equiv uh/v$, evaluated as follows:

$$f=\frac{6}{R_e'}\quad\left(R_e'\le 430\right) \tag{7a}$$

$$\sqrt{\frac{2}{f}}=A_s-\frac{1}{\kappa}\left[1-\ln\left(R_e'-\sqrt{\frac{f}{2}}\right)\right]\quad\left(R_e'>430\right) \tag{7b}$$

where $\kappa=0.41$, A_s= 5.5. A simple 0-equation model presented in eq. (9) was used to evaluate the depth-averaged Reynolds stress tensors (Kimura & Honda, 1997).

$$-\overline{u_i'u_j'}=D_h\left(\frac{\partial u_i}{\partial x_i}+\frac{\partial u_j}{\partial x_i}\right)-\frac{2}{3}k\delta_{ij},\quad D_h=\alpha hu_* \tag{8}$$

where α= empirical constant ($\alpha=0.5$ is used in this research); u*= local friction velocity ; and k = depth-averaged turbulent kinetic energy evaluated by the empirical formula proposed by Neze & Nakagawa (1993), who proposed the universal expression in equation (9) for turbulent kinetic-energy distribution

$$\frac{k}{u_*^2} = 4.78 \exp\left(-2\frac{z}{h}\right) \tag{9}$$

$$u_* \equiv \sqrt{f\left(u^2 + v^2/2\right)}$$

where z=direction perpendicular to the bottom bed. The depth-averaged turbulent kinetic energy becomes the following formula is $2.07u_*^2$ when equation (9) is integrated from the bottom to the surface.

$$k = 2.07u_*^2 \tag{10}$$

(q_{su}-w_0c_b) in the equations (4) and (5) means suspend and deposition of sediment. $\sin\theta_f$ and $\cos\theta_f$ can be calculated by

$$\sin\theta_f = \frac{|v|}{\sqrt{u^2+v^2}}, \cos\theta_f = \frac{|u|}{\sqrt{u^2+v^2}} \tag{11}$$

The additional term caused by the secondary currents S_{cx}, S_{cy} and S_{cs} are given as:

$$S_{cx} = C_{sn}\left[\frac{\partial \overline{u_x} A_n h \sin 2\theta}{\partial x} - \frac{\partial \overline{u_x} A_n h \cos 2\theta}{\partial y}\right] + C_{n2}\left[-\frac{\partial A_n^2 h \sin^2\theta}{\partial x} + \frac{\partial A_n^2 h \cos\theta \sin\theta}{\partial y}\right] \tag{18}$$

$$S_{cy} = C_{sn}\left[-\frac{\partial \overline{u_x} A_n h \cos 2\theta}{\partial x} - \frac{\partial \overline{u_x} A_n h \sin 2\theta}{\partial y}\right] + C_{n2}\left[\frac{\partial A_n \bar{c} h \sin\theta\cos\theta}{\partial x} - \frac{\partial A_n^2 h \cos^2\theta}{\partial y}\right] \tag{19}$$

$$S_{cs} = C_{cn}\left[-\frac{\partial A_n \bar{c} h \sin\theta}{\partial x} + \frac{\partial A_n \bar{c} h \cos\theta}{\partial y}\right] \tag{20}$$

The coefficient A_n means the magnitude of the secondary current. In the model neglecting the lag between the streamline curvature and the development of the secondary current, A_n is simply evaluated as:

$$A_n = \frac{\overline{u_s} h}{R} \tag{21}$$

where R: curvature radius of the streamline. Hosoda et al (2001) proposed a more sophisticated model, which takes into account the lag between the curvature and secondary currents. In this model, A_n is evaluated using a transport equation. Detailed descriptions of the model are given in the paper by Hosoda et al (2001). C_{s2}, C_{sn} and C_{n2} are model coefficients expressed with velocity profile functions as:

$$C_{s2} = \int_0^1 f_s(\zeta)^2 d\zeta \tag{22a}$$

$$C_{sn} = \int_0^1 f_s(\zeta) f_n(\zeta) d\zeta \tag{22b}$$

$$C_{n2} = \int_0^1 f_n(\zeta)^2 d\zeta \tag{22c}$$

where

$$u_s(\zeta) = \overline{u}_s f_s(\zeta), u_n(\zeta) = \overline{u}_n f_n(\zeta), \zeta = \frac{z}{h} \tag{23}$$

Hosoda et al (2001) derived the coefficients using velocity profiles proposed a model considering the change of velocity profile affected by the development of the secondary currents (Onda, 2004). Details of models are shown in each reference.

We consider the following 4 models.

Model 1: A plane 2D model without effects of secondary currents

Model 2: A plane 2D model with effects of secondary cur rents. The lag between the streamline curvature and the development of secondary currents are not included.

Model 3: A plane 2D model with effects of secondary cur rents. The lag between the streamline curvature and the development of secondary currents are considered.

Model 4: A plane 2D model with effects of secondary cur rents. The lag between the streamline curvature and the development of secondary currents as well as the change of mainstream velocity profile affected by the secondary currents are considered.

The governing equations in the Cartesian coordinate shown above are transformed into the generalized curvilinear form before application to real river flows. The detailed process of the transformation is available in Hosoda et al (2001).

2.2 *Numerical Scheme*

The governing equations are solved numerically using the finite volume method on a full staggered grid considering the conservativeness and compu-

tational stability. The grid has 70×30 grid-lines with grid cells of about $7\text{m} \times 7\text{m}$. (See Figure 5). 3 hours computation time for entire high flow period is performed using 4 models.

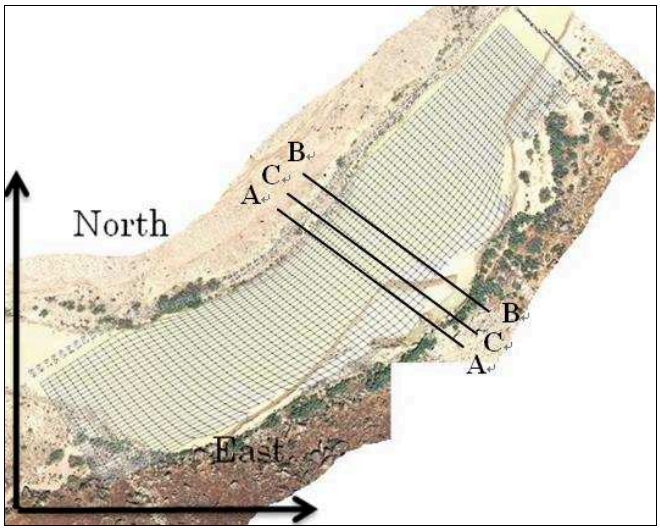

Figure 5 Computational grid

Table.1 Numerical conditions

i axis	70 meshes (7m)
j axis	30 meshes (7m)
Grain size	1.88mm
coefficient of roughness	0.0164
Water depth	Uniform flow depth is given at downstream end
Discharge (during flood)	1210 m^3/s
Downstream conditions for velocity	Gradient 0 condition $\frac{\partial u}{\partial \xi} = \frac{\partial v}{\partial \xi} = 0$
Side wall	Slip condition

3 RESULTS AND DISCUSSION

3.1 *Analysis on velocity vectors*

Figure 6 shows the time mean velocity vectors in the experimental and numerical results. In the numerical results, the colour contour of the velocity magnitude is shown together. In the result with model 1, there are two recirculations at left side bank though only one recirculation can be seen in the measured data. In each model 3 and 4, one recirculation is reproduced and the scale of the reproduce vortex is in good agreement with the measured result. When a recirculation occurs, the velocity near the bed goes toward the centre of the recirculation due to the generation of the secondary current. Such velocity near the bed cause a reaction force, which has effect to enlarge the scale of the recirculation. The comparison of the numerical results showed that the numerical model without effects of the secondary current may under-predict the horizontal scale of a recirculation. (See Figure.6)

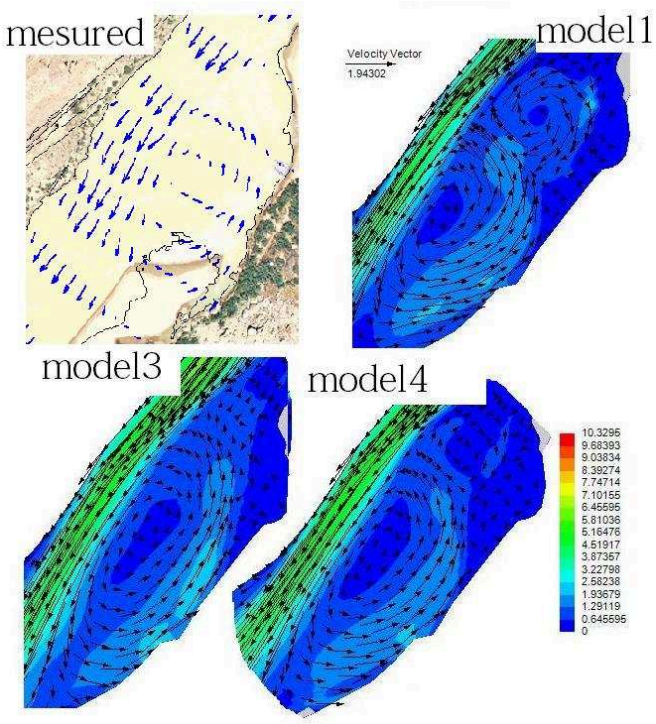

Figure 6 Time mean velocity vectors in the experimental result and numerical results with model 1, 3 and 4.

3.2 *Flow Velocity Distribution at the centre of the eddy*

Figure 7 shows the time-mean velocity profile across the section A-A shown in Figure 5. This line locates on the centre of the recirculation. The horizontal axis denotes the distance from the left bank and V denotes the velocity component perpendicular to the A-A section. The location of V=0 means the centre of the recirculation.

In the measured result, the location of V=0 is 60m from the left bank. In the computational results, this distance is 80m in model 1 and 60m in models 3 and 4.

All computational results generally replicated the velocity profile satisfactorily except the velocity around the peak near the left bank, where all models considerably over-predicted the maximum velocity. Through careful observation of computations, it is found that the numerical models with effects of the secondary current (models 3 and 4) could reproduce the velocity profile better than the model without effects of the secondary current. In the computations, we could not get a result with model 2 because the calculation with model 2 gets unstable. This is because the additional terms caused by the secondary currents like S_{cx}, S_{cy} and S_{cs} change rapidly near large scale vortexes which develop periodically at the interface. Around unsteady phenomena with separation vortexes, separation vortexes disappear before secondary currents fully develop and secondary currents also decay. It is pointed out that the model considering

the lag is necessary to get stable computational results for the flow phenomena with unsteady vortex shedding.

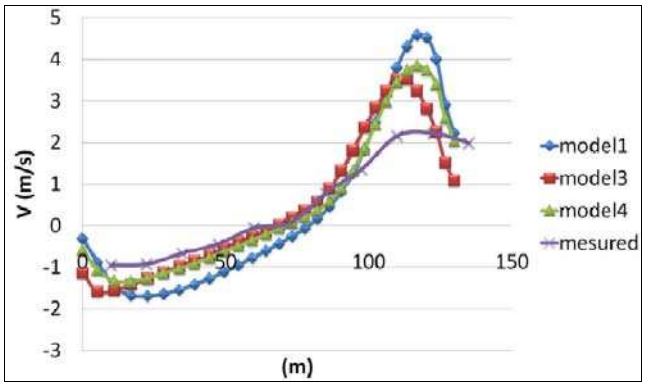

Figure 7 Abscissa axis means the distance from left bank.

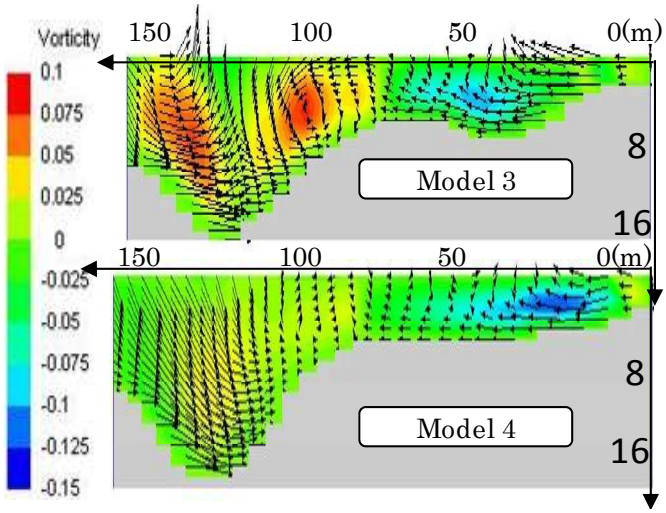

Figure 8 Section B-B in model 3 and C-C in model 4.

3.3 *Vertical flows at the centre of the eddy*

Figure 8 shows the velocity vectors and contour map of the vorticity at vertical sections along section B-B (model 3) and C-C (model 4). The sections B-B and C-C are chosen to go across the centre of the recirculation in each computational result. Those velocity patterns in vertical sections can be calculated using assumed velocity profiles and a three-dimensional continuity equation. In both result, a vortex in the clockwise direction can be seen near left bank and a vortex in the anti-clockwise direction can be seen near right bank. In the result by model 3, those two vortices show the generation of the secondary current of the first kind. The generation of the secondary current was simulated clearer in the result by model 3 than that by model 4. Model 4 includes the effect of the deformations of velocity profiles due to the generation of the secondary current. The deformation of the velocity profile has effect to suppress the development of secondary current due to the invers velocity profile near the surface. In other words, Model 3 can over-predict the secondary current. This seems to be the reason that the secondary current is clearer in the result by Model 4.

4 CONCLUSION

This paper presents the application of depth averaged plane 2D models with and without considering effects of the secondary currents to the field measurement data performed at the Colorado River, USA. 4 different types of depth averaged 2D models are applied. The comparison of the computational results and measurement data indicated that only the models considering effects of the secondary current could reproduce precisely the horizontal scale of the recirculating flow around a side-cavity. The computed flow patterns in a vertical section across the centre of the vortex contain a pair of vortices. The results imply that the depth averaged model including effect of the secondary current is a reasonable tool to predict flow structures in river flows with recirculation.

In the next steps, we should perform the computation under unsteady conditions and also should compute the sediment transport with bed deformations.

REFERENCES

Kimura, I., Onda, S., Hosoda, T,. & Shimizu, Y. 2009. 2D depth-averaged model for computing secondary current and its effect on suspended sediment transport in a side-cavity. JSCE, Vol.53 pp.1075-1080

Engelund, F. 1974. Flow and bed topography in channel bends, Proc. ASCE, J. Hydraulic Div., Vol.100, HY11, pp.1631-1647.

Hosoda, T. & Kimura, I. 1993. Vortex formations with free surface variation in the shear layer of plane-2D open channel flows. Proc, 9th Symp. on Turbulent Shear Flows, Kyoto Japan, Vol. 1, P112, pp.1-4.

Hosoda, T., Nagata, N., Kimura, I., Michibata, K. & Iwata, M. 2001. A depth averaged model of open channel flows and secondary currents in a generalized curvilinear coordinate system. Advances in Fluid Modeling & Turbulence measurements, (eds. H. Ninokata, A. Wada and N. Tanaka)

Kalkwijk, J.P. & de Vriend, H. J. 1980. computation of the flow in shallow river bends, J. Hydraulic Res., IAHR, Vol. 18, No.4, pp.327-342.

Kimura, I. & Hosoda, T 1997. Fundamental properties of flows in open channels with dead zone. J. Hydraulic. Engineer, ASCE, Vol.123 (2), pp.98-107.

Nagata, N., Hosoda, T., Nakato, T. & Muramoto, Y. 2005. Three dimensional numerical model for flow and bed deformation around river hydraulic structures. J. of Hydraulic Eng., ASCE, Vol.131, No.12, pp.1047-1087.

Nezu, I. & Nakagawa, H. 1993. Turbulence in Open-Channel Flows, IAHR Monograph, Belkema, Rotterdam, Netherlands.

Onda, S. 2004. PhD Thesis, Kyoto University.